

Observation of lattice distortion in the low-dimensional quantum spin system TiOBr by synchrotron x-ray diffraction - Evidence of spin-Peierls transition? –

Tomoyuki Sasaki, Masaichiro Mizumaki¹, Kenichi Kato^{1,2}, Yasuo Watabe, Yoshiki Nishihata, Masaki Takata^{1,2} and Jun Akimitsu

Department of Physics, Aoyama-Gakuin University, Sagamihara, Kanagawa 229-8558

¹*Japan Synchrotron Radiation Reserch Institute (JASRI), SPring-8, Mikazuki-cho, Sayo-gun, Hyogo 679-519*

²*CREST, Japan Science and Technology Corporation (JST), Kawaguchi, Saitama 332-0012*

(Received December 23, 2004)

We report here on physical properties and lattice distortion in the new quasi-one-dimensional spin system TiOBr by x-ray diffraction experiment using synchrotron radiation. Comparing the crystal structure between TiOBr and TiOCl, the difference of b -axis length plays a key role for physical properties in both systems. By using single crystal of TiOBr, superlattice reflections were observed at $(0\ 1.5\ 0)$ and $(0\ 2.5\ 0)$. The temperature dependence of superlattice reflections imply the first order transition at $T_{c1}=27\text{K}$. We analyzed the data using the simple dimerization model.

KEYWORDS: Spin-Peierls transition, lattice distortion, x-ray synchrotron radiation, crystal structure, dimerization

@ $S = 1/2$ Quantum Heisenberg Antiferromagnetic Chain (QHAC) is one of the best candidate to investigate a role of quantum spin fluctuations. A small perturbation to QHAC causes a drastic change of the ground state with spontaneous broken symmetry. The spin-Peierls state being coupled with phonons results in a new disordered ground state with a finite energy gap for the excitation spectrum, accompanying a spontaneous dimerization of the spin and the lattice.

The inorganic compound CuGeO_3 has proven to be a first inorganic spin-Peierls system and a lot of works, both theoretical and experimental, has been devoted to this material.^{1,2} After the discovery of this material, impurity effect on the spin-Peierls compound was examined.³ Neutron scattering experiments on $\text{CuGe}_{0.993}\text{Si}_{0.007}\text{O}_3$ demonstrated the coexistence of the Bragg spot intensities for both lattice dimerization and antiferromagnetic (AF) orderings at low temperature.⁴ The two Bragg spots are resolution limited, which implies that the two orderings are truly long ranged. The result was very surprising since the two orderings had been shown to be exclusive in homogeneous systems. A theoretical proposal was presented for understanding of this remarkable phenomenon using phase Hamiltonian technique at $T =$

OK.⁵ This fact suggests that a new phenomenon can be created by a new perturbation such as orbital and charge degrees of freedom.

Recently, the layered compound TiOCl has been suggested to be a new spin-Peierls system with one-dimensional (1D) orbital ordered array, by which 1D chain composes.⁶ This material has long been believed to be a $S=1/2$ two-dimensional antiferromagnet because of the layered structure and having a very small and temperature independent magnetic moment,⁷ which suggests that the ground state is the Resonating-Valence-Bond (RVB) state in the Mott-insulator.

The structure of TiOCl is of FeOCl type, where the TiO_4Cl_2 bilayers separate from each other along c -axis. The distorted TiO_4Cl_2 octahedra build an edge-shared network. The nearest-neighbor Ti ions form a staggered site by $a/2$ and $b/2$ between each layer along the a - and b -axis. The next-nearest-neighbor Ti ions form an edge-shared Ti ion along b -axis in the same plane. The most important exchange path is direct t_{2g} orbital overlap, rather than superexchange interaction. In this case, the chains are expected to form along a - or b -axes [see Fig.1 b) and c) in Ref.⁶]. However, by comparing ESR measurements to angular overlap model (AOM)⁸ and by generalized gradient approximation (GGA) which suggests that TiOCl is subject to large orbital fluctuations driven by the electron-phonon coupling,⁹ a uniform $S = 1/2$ chains are suggested to form along b -axis because of the occupied Ti d_{xy} orbital. The temperature dependence of susceptibility can be fitted using $S = 1/2$ Bonner-Fisher curve with an exchange constant of $J = 660\text{K}$, and can be observed a sharp drop at $T_{c1} = 67\text{K}$ and a pronounced kink at $T_{c2} = 95\text{K}$. It was also observed by the NMR measurement that the opening of the pseudo-spin gap at $T^* \sim 135\text{K}$.¹⁰ The pseudo-spin gap energy was evaluated to be $\Delta_{\text{NMR}} \sim 430\text{K}$ by NMR¹⁰ and $2\Delta_{\text{opt}} \sim 430\text{K}$ by optical measurement below T_{c1} .^{11,12} In spite of such a large pseudo-spin gap, the phase transition is suppressed by a strong coupling between spin and lattice degrees of freedom and orbital fluctuation, and as the result, is realized the spin gap state at T_{c1} . TiOCl is possible to be an 1D system by the formation of the orbital ordering along b -axis, and finally the system causes the spin-Peierls instability driven by the electron-phonon interaction.

It is expected that the 1D nature in TiOBr is weaker than that in TiOCl, because the lattice parameter ratio (a -axis/ b -axis) in TiOBr is smaller than that in TiOCl. Actually, physical properties of 1D nature obtained by the temperature dependence of susceptibility in TiOBr are proportionally weaker than that in TiOCl.¹³ Although the measurement for possible structural phase transition has been examined by x-ray and neutron powder diffraction, it has not yet been found.

In this letter, we present the observation of the superlattice reflections probably due to the spin-Peierls transition by the SR x-ray diffraction in the low dimensional quantum spin system TiOBr.

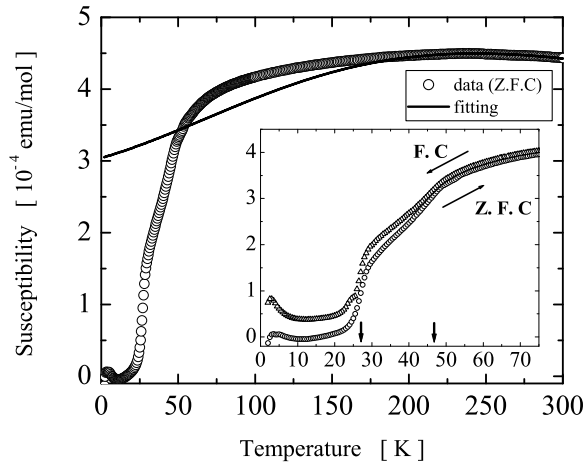


Fig. 1. Temperature dependence of susceptibilities for polycrystalline TiOBr in a magnetic field of 5.5 T without Curie term subtraction. Arrows indicate magnetic transition temperatures T_{c1} and T_{c2} . The solid line indicates the fitting result with Bonner-Fisher curve. The inset is emphasized at low temperature region.

Polycrystalline and single crystal samples of TiOBr were synthesized from Ti, TiO₂ and TiBr₄ by the chemical vapor transport method.^{6,13,14} The precursors of TiOBr were prepared from a pellet of Ti/TiO₂ (1:2 by mol) and sextuple TiBr₄. In the evacuated sealed quartz tube, there were a pellet of TiBr₄ at the cooled zone and of Ti/ TiO₂ at the hot zone, where both were heated up to 700 with a gradient at 100 within 20 cm. It takes 3 days to cool down from 700 to 450. The excess TiBr₄ was carried away at cooled zone. The rectangle single crystal ($2 \times 10 \times 0.04$ mm) was grown in *ab* - plane, and the major axis corresponds to *b*-axis.

The polycrystalline samples were characterized by the x-ray powder diffraction, which showed a small amount of Ti₂O₃ phase. To characterize the single crystal, the x-ray powder diffraction, EPMA and Laue technique were employed, which shows no evidence of impurity phase and its composition being stoichiometric.

Magnetic susceptibility was measured using a DC SQUID magnetometer (MPMSR2, Quantum Design) at 5.5 T. For precise crystal structure determination, SR x-ray powder diffraction experiments were carried out by large Debye-Scherrer camera installed at BL02B2, SPring-8.¹⁵ The exposure time of x-ray was 160 min. The x-ray patterns were measured at 300K, 37K and 12K. The wavelength of incident x-ray was 0.922Å. The obtained powder data were analyzed by the Rietveld method. To determine the lattice distortion, SR single crystal diffraction experiments were carried out on the four-circle diffractometer at BL46XU, SPring-8. The x-ray wavelength using Si (111) monochromators was 1.0332Å. The size of single crystal is about $1.5 \times 6 \times 0.02$ mm³, which mountains onto refrigerator with the (h k 0)

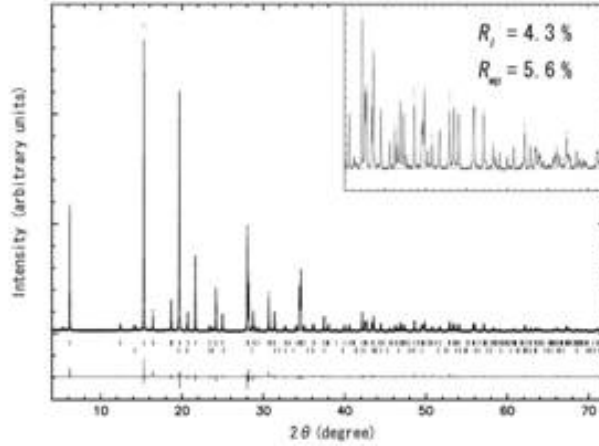


Fig. 2. Rietveld analysis of the x-ray diffraction pattern for polycrystalline TiOBr being fitted for the orthorhombic $Pm\bar{m}n$ model. The data were taken at 300K, in which several weak impurity peaks were found and identified as Ti_2O_3 .

(a)

	x	y	z	$B(\text{\AA})$
Ti	0.25(0)	0.75(0)	0.10951(7)	0.33(1)
O	0.25(0)	0.25(0)	0.95151(27)	0.22(5)
Br	0.25(0)	0.25(0)	0.32723(6)	1.18(2)

Space Group $Pm\bar{m}n(59:2)$ $Z = 2$

(b)

	a	b	c
300K	3.78458(2)	3.48528(2)	8.52520(5)
37K	3.78014(51)	3.46647(7)	8.49861(69)
12K	3.78307(36)	3.46556(9)	8.49643(57)

The factor of parameter are \AA

Table I. (a) Atomic parameters for TiOBr obtained from synchrotron x-ray diffraction at 300K. The space group is $Pm\bar{m}n$. (b) Lattice parameters at 300, 37 and 12K.

reciprocal plane parallel to the χ -axis.

In Fig. 1, the susceptibility data for TiOBr were obtained from the polycrystalline samples. Although the temperature dependence of susceptibility in TiOBr resemble that in $TiOCl$,^{6,8} we observed a small hysteresis curve in TiOBr due to a different cooling process (field cooling and zero field cooling processes) below 280K. The data in Fig. 1 are subtracted the Van-Vleck

	a [Å]	b [Å]	c [Å]	T_{c1}	T_{c2}	J [K]	Δ/k_B
TiOBr	3.785	3.485	8.525	27	47	188	149
TiOCl	3.789 ⁸⁾	3.365 ⁸⁾	8.060 ⁸⁾	67 ⁶⁾	95 ⁶⁾	660 ⁶⁾	440 ¹⁰⁾

	Ti-Ti(a) [Å]	Ti-Ti-Ti(a) [°]	Ti-Ti(b) [Å]	Ti-Ti-Ti (b) [°]
	3.1787	73.07	3.4853	180
	3.1811	73.10	3.3650	180

Table II. The summarized physical properties in TiOBr and TiOCl. The lower column shows the distances and angles between the nearest-neighbor Ti atoms in zig-zag chain along a -axis and linear chain along b -axis suggested by Seidel *et al.*⁶

susceptibility (χ_0) and the Curie term of Ti^{3+} below 20K from the raw data. The Curie term is originated from the paramagnetic (PM) component in Ti_2O_3 due to the deterioration and the unpaired free $S = 1/2$ spins with the finite chain effects. The Curie term is order of $0.8\%/Ti^{3+}$, and the χ_0 is 1.3×10^{-5} emu/mol. The data above 220K are fitted to the Bonner-Fisher curve¹⁶ with the nearest -neighbor exchange $J = 188K$ and the g factor of 1.752. The g factor was obtained from the ESR measurement.¹³ The data between 10 and 20K are fitted to the function of Troyer *et al.* who suggested that the susceptibility of the spin gap system decreases as $aT^{-1/2}\exp(-\Delta/k_B T)$ at sufficiently low temperature ($T \ll \Delta/k_B$),¹⁷ which gives the energy gap $\Delta/k_B = 149K$. The data shown in the inset of Fig. 1 features a rapid drop of the susceptibility at $T_{c1} = 27K$ and $T_{c2} = 46K$, which are defined by the value of the differentiated susceptibility. In addition, we observed the third anomaly around 10K (T_{c3}) at which susceptibility increases again with decreasing temperature. The ratio $2\Delta/k_B T_{c1,c2} = 6.5\sim 11$ is smaller than $2\Delta/k_B T_{c1,c2} = 9\sim 13$ of TiOCl,¹⁰ and these values are much larger than 3.5 expected from BCS theory.

Figure 2 shows the Rietveld analysis of the SR x-ray diffraction pattern for polycrystalline TiOBr at 300K for which the orthorhombic $Pm\bar{m}n$ model was fitted. Table.1 shows atomic parameters at 300K and its lattice parameters at 300, 27 and 12K. It was finally confirmed that the TiOBr has a same crystal structure with that of TiOCl.¹⁸ Our x-ray diffraction analysis shows that the structural difference between TiOBr and TiOCl is mainly its lattice parameter. From the temperature dependence of the structural analysis, superlattice reflection due to lattice distortion was not observed between the lowest temperature and room temperature. This is probably due to the weak intensity of the superlattice reflection in the powder reflection data. However, lattice parameters decrease with decreasing temperature, in particular b -axis drastically changes, which confirms the development of intra-interaction with decreasing temperature.

Table 2 shows the summary of the physical properties both in TiOBr and TiOCl. As

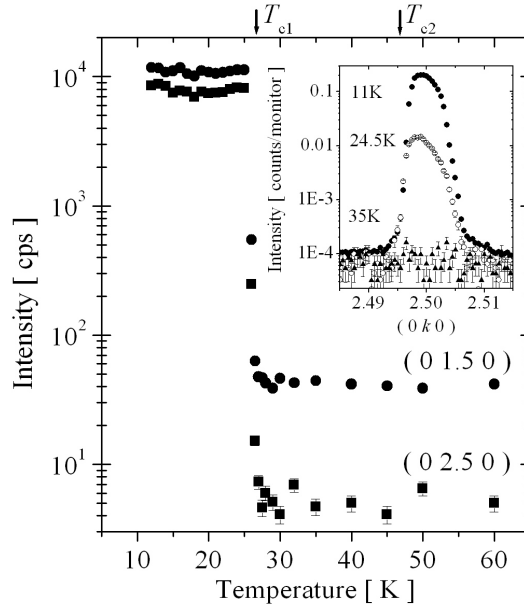


Fig. 3. Temperature dependence of the superlattice reflections at (0 1.5 0) and (0 2.5 0) on heating process. The inset shows the peak profiles of the (0 2.5 0) reflection.

shown in Table 2, roughly speaking, the value of the physical properties in TiOBr are 30-50% smaller than these of TiOCl. This corresponds that b -axis in TiOBr is longer than that in TiOCl, namely the intra-chain exchange in TiOBr is weaker than that in TiOCl. Moreover, although there is no significant difference of Ti-Ti distance along a -axis between TiOCl and TiOBr, the Ti-Ti distance along b -axis is significantly different between them.

Seidel *et al.* interpreted the abrupt drop of the susceptibility at T_{c1} (=67K) as a transition into a spin-Peierls state⁶ in TiOCl. We have clearly observed the broad anomalies in heat capacity at T_{c1} and T_{c2} , and change of the relaxation rate in μ SR and of ESR signal under high magnetic field at T_{c1} , T_{c2} and T_{c3} .^{19,20}

What is happened at T_{c1} in this system? In order to search the superlattice reflections, we have performed a precise x-ray scattering measurement by using the single crystal of TiOBr. Consequently, we observed superlattice reflections at (0 1.5 0) and (0 2.5 0) by SR x-ray diffraction, which evidenced the lattice distortion in single crystal of TiOBr. The temperature dependence of intensities of superlattice reflections (0 1.5 0) and (0 2.5 0) are shown in Fig.3. With increasing temperature, the intensities gradually decreased, and suddenly dropped at T_{c1} . Although it is not shown in Fig.3, this phase transition has thermal hysteresis around T_{c1} , suggesting that this transition is of first order. Although the intensities above T_{c1} are small, the intensities seem to still survive between T_{c1} and T_{c2} .

Degree of lattice distortion (δ) was estimated from the superlattice reflections. The intensities of (0 1.5 0) and (0 2.5 0) reflections were normalized by (0 2 0) main reflection. Since

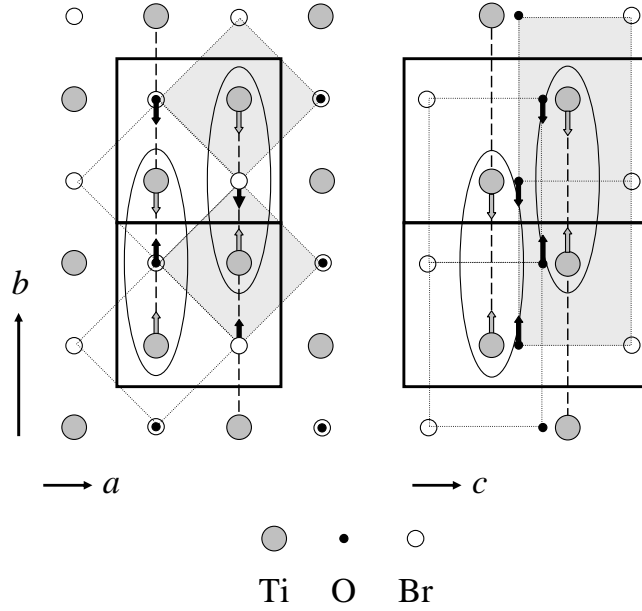


Fig. 4. Atomic shifts at 11K in TiOBr. The figure shows the model in which Ti and O atoms are shifted. Bold frame indicates the unit cell at high temperature, and the new unit cell are doubled along b -direction. Dashed frame indicates TiO_4Br_2 octahedra, of which color shows the different layer each other. Arrows indicate the directions of shifts.

only two reflections were observed, we employed the simplest model in which only Ti atoms are shifted. This model, unfortunately, can not explain the intensity ratio between $(0\ 1.5\ 0)$ and $(0\ 2.5\ 0)$. Next model is that all atoms along b -axis are shifted with same value. In order to simplify the model we employ the three types of shifts, i.e. (a) three kind of atoms, (b) two kind of atoms, and (c) one kind of atom, and totally six type models are analyzed for this estimation. Fig.4 shows that Ti and O atoms shifts along b -axis for example. This simple estimation supports two models; one is that Ti and O atoms are shifted with $\delta_{\text{Ti,O}} = 0.0022 \pm 0.0002$, and the other is that only O atom is shifted ($\delta_{\text{O}} = 0.0161 \pm 0.0016$). The unit is given as doubled unit cell ($b' = 2b$) in reciprocal lattice unit. In both cases, the shift of O atoms plays a key role for the estimation. Assuming that 1D chains are aligned along b -axis, d_{xy} orbital in Ti atom should be occupied by $3d$ electron,⁶ i.e. Ti atoms centered in TiO_2Br_2 ribbon are arrayed along b -axis (see Fig.4 right picture).

In summary, we have reported the magnetic properties and structural analysis in TiOBr. From the structural analysis, we found that TiOBr has a similar crystal structure with that of TiOCl except a large difference of b -axis length, as shown in Table 2. However, we emphasize here that the b -axis difference substantially affect the one dimensionality for both systems. From the single crystal x-ray diffraction measurements, we clearly observed the superlattice reflections along b -axis, which is of first order transition. We tried to fit the intensities of the superlattice reflection to the simple dimerization model as shown in Fig.4. More detailed

experiment for the crystal structure determination is now in progress which will be published in near future.

We would like to thank S. Kimura (Spring-8) for technical supports, and T. Yokoo (KEK) for his interest in this work and for fruitful discussion. Aoyama-Gakuin group was partly supported by 21st COE program, "High-Tech Reserch Center" Project for Private Universities: matching fund subsidy from MEXT (Ministry of Education, Sports, Culture, Science and Technology), 2002-2004 and Grant-in-Aid for Scientific Research on Priority Area Ministry of Education, Sports, Culture, Science and Technology of Japan. The synchrotron radiation experiments were performed at the BL02B2 and BL46XU (R04B46XU-0020N) in the SPring-8 with the approval of the Japan Synchrotron Radiation Research Institute (JASRI)

References

- 1) M. Hase, I. Terasaki and K. Uchinokura: Phys. Rev. Lett. **70** (1993) 3651
- 2) M. Nishi, O. Fujita and J. Akimitsu: Phys. Rev. B **50** (1994) 6508
- 3) M. Hase, I. Terasaki, Y. Sasago, K. Uchinokura and H. Obara: Phys. Rev. Lett. **71** (1993) 4059
- 4) L. P. Regnault, J. P. Renard, G. Dhahlenne and A. Revcolevschi: Europhys. Lett. **32** (1995) 579
- 5) H. Fukuyama, T. Tanimoto and M. Saito: J. Phys. Soc. Jpn. **65** (1996) 1182
- 6) A. Seidel, C. A. Marianetti, F. C. Chou, G. Ceder and P. A. Lee: Phys. Rev. B **67** (2003) 020405(R)
- 7) R. J. Beynon and J. A. Wilson: J. Phys.:Condens. Matter **5** (1993) 1983
- 8) V. Kataev, J. Baier, A. Moller, L. Jongen, G. Meyer and A. Freimuth: Phys. Rev. B **68** (2003) 140405(R)
- 9) T. Saha-Dasgupta, R. Valenti, H. Rosner and C. Gros: Europhys. Lett. **67** (2004) 63
- 10) T. Imai and F. C. Chou: cond-mat/0301425 (2003)
- 11) P. Lemmens, K. Y. Choi, G. Caimi, L. Degiorgi, N. N. Kovaleva, A. Seidel and F. C. Chou: Phys. Rev. B **70** (2004) 134429
- 12) G. Caimi, L. Degiorgi, N. N. Kovaleva, P. Lemmens and F. C. Chou: Phys. Rev. B **69** (2004) 125108
- 13) C. Kato, K. Tsuchida, Y. Kobayashi and M. Sato: J. Phys. Soc. Jpn. **74** (2005) 473
- 14) H. G. v. Schnering, M. Collin and M. Hassheider: Z. Anorg. Allg. Chem. **383** (1972) 137
- 15) E. Nishibori, M. Takata, K. Kato, M. Sakata, Y. Kubota, S. Aoyagi, Y. Kuroiwa, M. Yamakata and N. Ikeda: Nuclear Instruments and Methods in Physics Research A, 467 (2001) 1045
- 16) W. E. Hatfield: J. Appl. Phys. **52** (1981) 1985
- 17) M. Troyer, H. Tsunetsugu and D. Wurtz: Phys. Rev. B **50** (1994) 13515
- 18) H. Schafer, F. Wartenpfehl and E. Weise: Z. Anorg. Allg. Chem. **295** (1958) 268
- 19) T. Sasaki, Y. Nishihata, H. Takagiwa, S. Kuroiwa, K. Ohishi, W. Higemoto, A. Kouda, Y. Kadono and J. Akimitsu: to be published
- 20) S. Kimura, T. Sasaki, K. Kindo and J. Akimitsu: to be published